

Industrial processes control with the use of a neural tomographic algorithm

Abstract. This paper presents the original Electrical Impedance Tomography (EIT) imaging algorithm in relation to physico-chemical processes of crystallization. Thanks to the developed method based on artificial neural networks (ANN), it was possible to develop an algorithm that could allow effective detection of crystals and other inclusions inside the reactor filled with non-Newtonian fluid. The neural controller contains a structure of independent neural networks. The number of ANNs corresponds to the resolution of the output image mesh.

Streszczenie. W artykule przedstawiono oryginalny algorytm obrazowania z wykorzystaniem elektrycznej impedancji tomograficznej (EIT) w odniesieniu do fizykochemicznych procesów krystalizacji. Dzięki opracowanej metodzie opartej na sztucznych sieciach neuronowych (SSN) możliwe było opracowanie algorytmu, który umożliwiłby skuteczne wykrywanie kryształów i innych wtrąceń wewnątrz reaktora wypełnionego płynem nienuetonowskim. Sterownik neuronowy składa się z systemu niezależnych sieci neuronowych. Liczba SSN odpowiada rozdzielczości siatki obrazu wyjściowego. (Sterowanie procesami przemysłowymi z wykorzystaniem neuronowego algorytmu tomograficznego).

Keywords: industrial tomography; electrical impedance tomography; artificial neural networks; machine learning

Słowa kluczowe: tomografia przemysłowa; elektryczna tomografia impedancyjna; sztuczne sieci neuronowe; uczenie maszynowe

Introduction

Process tomography is picking up in significance alongside innovative advancement [1], [2]. At present, a significant trend can be watched for the robotization of modern procedures, which is firmly identified with process control. The need to automate the control of innovative procedures is one of the fundamental purposes behind the dynamic improvement of IT information handling strategies [3], [4]. Simulation and experimental tests are an important condition for optimizing the control of processes carried out by liquid and suspension mixing systems that under certain circumstances can crystallize [5]. An example of such a substance is biodiesel.

Common measurement tools used to quantify physico-chemical processes, such as sensors and markers, are often characterized by evaluation capabilities limited to specific points. Due to the high degree of difficulty in modeling the mixing and heating processes of crystallizing substances [6], which are characterized by a distinct non-Newtonian flow, traditional Computational Fluid Dynamics models do not provide a suitable basis for dimensioning mixing and heating systems, and therefore become useless. Classical models do not take into account granulometric parameters. The method of determining the rheological properties of liquids is difficult. In addition, traditional models used to simulate the mixing and heating of multiphase systems are still inaccurate [7], [8]. This fact may lead to misinterpretations, especially with regard to modeling and simulation of mixing and heating processes of non-Newtonian liquids, viscous and loaded with foreign particles. For this reason, reliable forecasts regarding the course of such processes are virtually impossible.

The above-mentioned problems are an important reason to intensify efforts to develop an effective method of monitoring and supervising liquid crystallization processes [9]. Electrical impedance tomography (EIT) is a modality with high application potential [10]. It was assumed that having an appropriate tomograph, you can effectively monitor the course of physico-chemical processes, especially in the field of crystal formation in reactors or other similar tanks. Industrial processes are dynamic. Parameters such as temperature or stirring speed can be controlled over time. Thanks to the constant regulation of the above process parameters, you can keep the liquid in a completely liquid state, without inclusions and crystals, and

at the same time minimize the cost of electricity consumption by reducing or eliminating maintenance activities to the necessary minimum. For example, if a given type of liquid should not be overheated, then the intensity of mixing at a lower temperature can be increased. In turn, fluids that can be heated can be less mixed. The effect will still be the same - prevention against the precipitation of crystalline structures. Adaptive industrial process control can be implemented using the appropriately selected EIT algorithm.

There are many methods for solving numerical problems [11,12]. The main goal of the presented research is to develop an EIT controller built from many cooperating neural networks [13]. ANNs based on multilayer perceptrons were used in the study, which implied a supervised way of training the neural networks. For this reason, the presented method is included in the group of machine learning techniques [14], [15]. The task of the neural controller is to convert the input values of electrical signals into individual points of the reconstructed output image. The specific design of the controller makes the tomographic image output is generated pixel by pixel. Thanks to this, the image obtained at the exit quite well reflects the actual cross-section of the object under study [16]. The structure of the algorithm consisting of many separate neural networks makes it sensitive even to small inclusions contained in the liquid. Image resolution is also high.

Method and model

In this chapter a neural model enabling efficient reconstruction of tomographic images was presented. The model of reactor was filled with liquid. The simulation model could undergo crystallization because of changing physico-chemical conditions. The main task of the EIT controller was crystals identification that were formed in the liquid.

A distinctive feature of the presented model is the separate training of multiple neural networks in an amount equal to the resolution of the mesh of output images. The input vector of electrical measurements generated by 16 electrodes placed around the reactor had 96 values of voltage drops. The resolution of the image output matrix was 2883 pixels. Each shade of the color displayed in a given element of the image mesh corresponds to a specific conductance value of the examined cross-section of the

real object. A schematic model of a tomography system based on multiple neural networks is shown in Fig. 1.

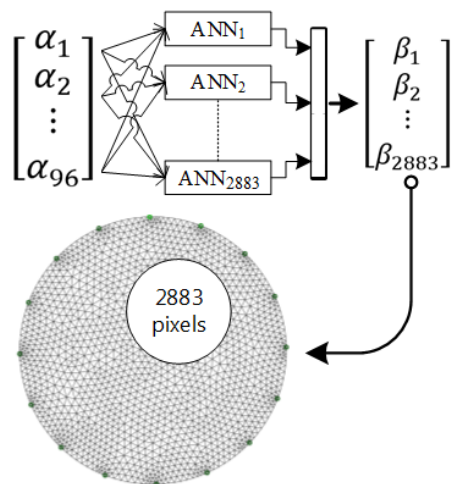


Fig.1. A mathematical neural model for converting electrical signals into images

Table 1 presents the method of dividing all data into three sets: training set, validation set and test set in the proportions: 70%, 15%, 15% respectively. In addition, Table 1 also contains the results of the network learning process for a single pixel of the output image. The MSE (square root error) test set is a commonly used indicator of network learning quality. The smaller the MSE, the higher the quality of the network. If the R (regression) coefficient is close to 1, the fidelity of mapping of the neural network is high. R reflects the level of correlation between forecasting results and references. In the discussed case, MSE is low and R is relatively high. This proves a good quality of trained ANN.

Table 1. Division of data into the sets and results of the training process

	Samples	MSE	Regression (R)
Training	24500	0.0254666	0.820920
Validation	5250	0.0289041	0.798704
Testing	5250	0.0285931	0.816868

Fig. 2 shows the laboratory model of reactor. In the upper part of the bucket a specially designed installation was placed. This frame enables the suspension of pipe-shaped elements immersed in water. Those elements are filled with powdered substance of a different conductance than the liquid in which they are immersed.



Fig.2. The physical model of the reactor – top view (left) and side view (right)

A suitable upper frame structure allows adjustment of the position of the tubular containers both relative to the reactor and relative to each other. You can also change the number of tubes immersed in a bucket. Around the reactor there are 32 sockets prepared for connecting the electrodes around the reactor. In the described tests, 16 electrodes were connected to the reactor using every other socket. Using the finite element method and the results of

measurements obtained thanks to the physical model, a simulation algorithm was developed with the help of which 35,000 training cases were generated.

Fig. 3 shows a schematic of a single neural network generating a real number on the output. The value of the ANN output corresponds to the predicted conductivity of a given pixel on the reconstructed tomographic image grid. The structure of the neural network is MLP (multi-layer perceptron) with 96 input neurons, 1 hidden layer with 14 neurons in the hidden layer and the one-neuron output layer. It is a regressive network.

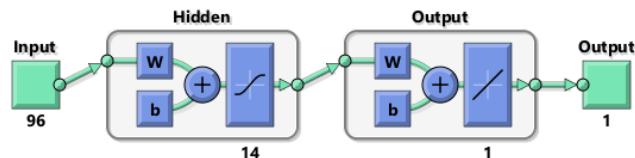


Fig.3. ANN that generates a single point of the output image

Fig. 4 presents the course of the neural network training process. Each of the 3 lines indicate MSE values in particular iterations. Training was completed in the epoch of 64 after the MSE for validation set had not decreased in the 6 consecutive iterations. Fig. 4 corresponds to the MSE and R values shown in Table 1.

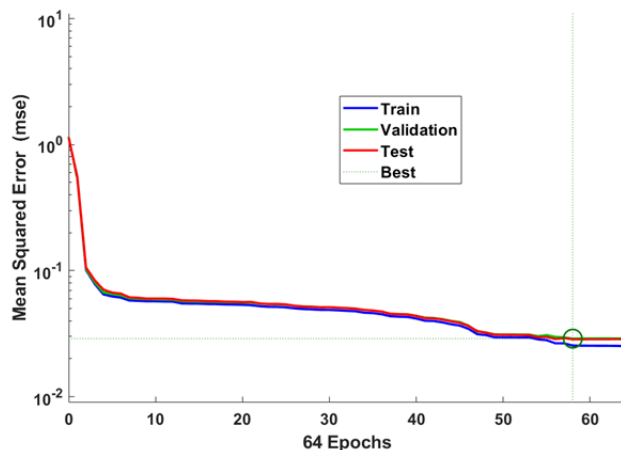


Fig.4. Best validation performance (MSE=0.0289 at epoch 58)

Fig. 5 shows the regression statistics for the testing set. The R=0.816868 indicator corresponds to Table 1. The dotted line indicates the perfect match. The solid line corresponds to the averaged reconstructions obtained thanks to the multiply neural controller.

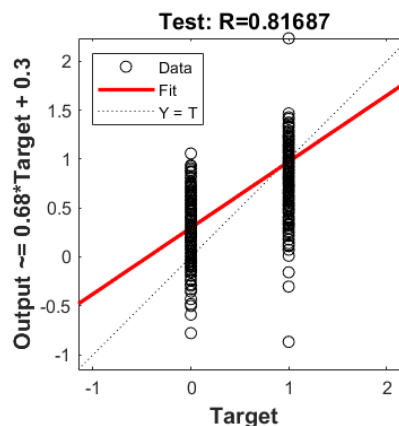


Fig.5. Best performance for testing set

Results

Fig. 6 and Fig. 7 present the results of a tomographic reconstruction of the selected case. Both figures have been divided into three parts. The upper parts present the reference images. It is important that the presented cases are reconstructions carried out on the testing set, which means that the presented measurements did not participate in the process of neural networks training.

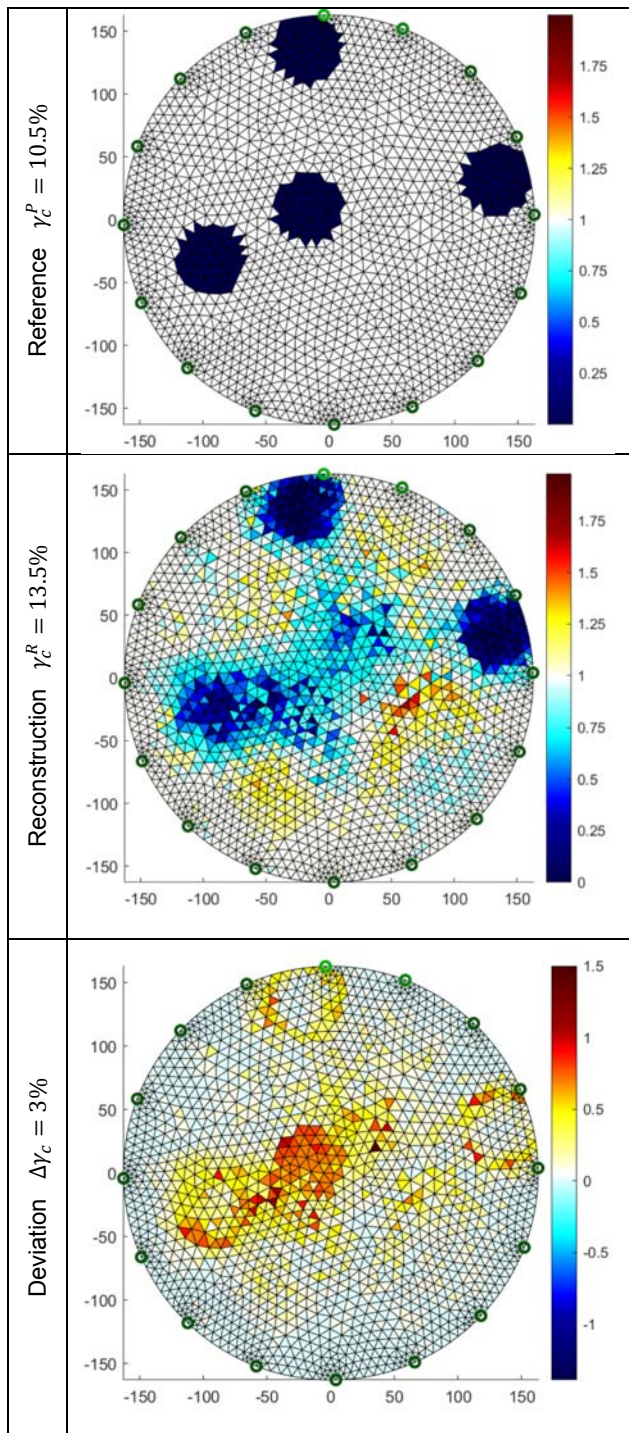


Fig.6. EIT reconstruction example for 4 crystals

Fig. 6 shows 4 large crystals visibly contrasting with the bright background. The positioned next to the drawing color bar allows to read the conductance values of specific image pixels. The conductance of background equals 1, while the conductance of pure crystals is close to 0. Effective supervising the crystallization process needs information on

the degree of crystallization of the tested substance at a given time. To allow this, the percentage crystallization coefficient γ_c was created. It is calculated according to the formula (1).

$$(1) \quad \gamma_c = \frac{l}{L} \times 100\%$$

where: l – the number of mesh pixels denoting crystallization, L – the mesh resolution

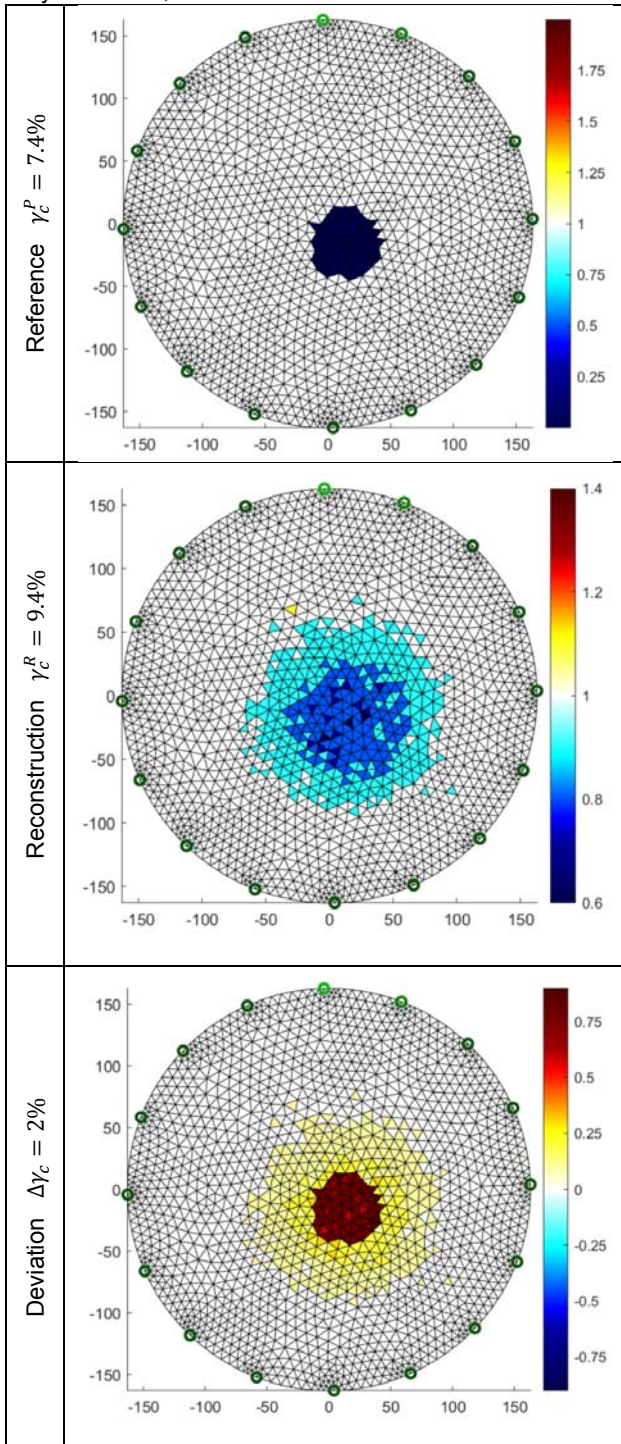


Fig.7. EIT reconstruction example for 1 central crystal

Moreover, in order to enable a good comparison of the tomographic reconstruction with the reference (pattern), the quantitative crystallization coefficient deviation $\Delta\gamma_c$ was defined (2).

$$(2) \quad \Delta\gamma_c = |\gamma_c^P - \gamma_c^R|$$

where: γ_c^P – crystallization coefficient for given pattern,
 γ_c^R – crystallization coefficient for proper reconstruction.

In the second part of Fig. 6 and Fig. 7 you can see a reconstructed tomographic images created using a neural algorithms. Crystallization coefficient for 4-crystals reconstruction is $\gamma_c^R = 13.5\%$ and for 1-crystal reconstruction is $\gamma_c^R = 7.4\%$. Comparing the crystallization coefficients γ_c (for pattern) with γ_c^R (for reconstructions) we obtain a deviations respectively $\Delta\gamma_c = 3\%$ (for 4-crystals) and $\Delta\gamma_c = 2\%$ (for 1-crystal).

Fig. 8 presents a histogram of deviations with Pareto line for the 1-crystal case (see Fig.7). The sorted histogram with Pareto line contains 5 bins of deviation $\Delta\gamma_c$ values that was sorted in descending order. The solid line denotes the total percentage of considered cases. The Pareto chart was created to highlight the most important factors in the considered data set. In this histogram those important factors are deviation values $\Delta\gamma_c$ for individual measuring cases. The Pareto chart is one of the most important quality control tools that helps to identify problems.

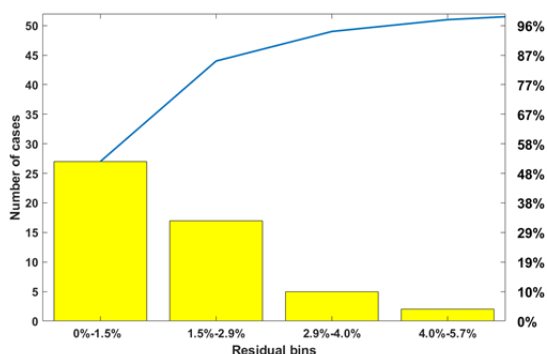


Fig.8. Deviations histogram with Pareto line for 1-crystal case

In Fig. 8 the Pareto line shows that $(27 + 17) / 50 \approx 88\%$ of the deviations $\Delta\gamma_c$ come from 2 out of 5 = 40% bins. It could be noticed that in this case Pareto principle applies rather roughly.

Conclusion

The research results presented in this paper show that the use of a multiple EIT neural system to control crystallization processes can be effective. During the research, a neural network system that allows the reconstruction of tomographic images intended for the detection of crystals formed in a liquid filled reactor was developed.

The logged indicators of the learning process of the selected neural network are the basis for stating that the developed neural tomography algorithm has the generalization ability. The developed algorithm is able to effectively reconstruct cases measured by the EIT method, which have not yet occurred in the set of training cases. This is a very valuable and desirable feature of the controller.

The above predictions have been confirmed during numerous simulation experiments. The examination of the accuracy of the EIT predictor included several dozen cases that did not participate in the ANN training process. Two of those cases were illustrated in Fig. 6 and Fig. 7. Visual analysis of the chosen cases allow to accomplish that the reconstructions have some errors. However, they are not large enough to significantly distort the actual state of the investigated process.

A crystallization coefficient for reconstruction γ_c was developed. The above coefficient was defined in order to estimate the degree of liquid crystallization in the reactor.

The quantitative nature of this parameter enables its use for the automation of technological processes. After calculating the separate mean deviations $\overline{\Delta\gamma_c}$ for all cases used for testing, it turned out that generalized mean deviation $\overline{\Delta\gamma_c} = 1.7\%$. Therefore, having the large number of measurements, the mean deviation from the reference cases is small. This fact indicates a high potential for application of the neural tomographic algorithm.

Authors: Tomasz Rymarczyk, Ph.D. Eng., University of Economics and Innovation, Projektowa 4, Lublin, Poland / Research & Development Centre Netrix S.A. E-mail: tomasz@rymarczyk.com; Grzegorz Kłosowski, Ph.D. Eng., Lublin University of Technology, Nadbystrzycka 38A, Lublin, Poland, E-mail: g.klosowski@pollub.pl; Tomasz Cieplak, Ph.D., Lublin University of Technology, Nadbystrzycka 38A, Lublin, Poland, E-mail: t.cieplak@pollub.pl; Edward Kozłowski, Ph.D., Lublin University of Technology, Nadbystrzycka 38A, Lublin, Poland, E-mail: e.kozlovski@pollub.pl;

REFERENCES

- [1] Rymarczyk T., Kłosowski G., Cieplak T. and Kozłowski E., Application of a neural EIT system to control the processes, PTZE — 2018 Applications of Electromagnetic in Modern Techniques and Medicine, 09-12 September 2018, Raclawice, Poland.
- [2] Ziolkowski M., Gratkowski S., Zywicka A. R. Analytical and numerical models of the magnetoacoustic tomography with magnetic induction. *COMPEL - Int. J. Comput. Math. Electr. Electron. Eng.* 37 (2018), 538–548
- [3] Kosicka E., Kozłowski E., Mazurkiewicz D., Intelligent Systems of Forecasting the Failure of Machinery Park and Supporting Fulfilment of Orders of Spare Parts. (2018), 54–63
- [4] Gola A., Nieoczym A., Application of OEE Coefficient for Manufacturing Lines Reliability Improvement. in *Proceedings of the 2017 International Conference on Management Science and Management Innovation (MSMI 2017)* (Atlantis Press, 2017), 189–194
- [5] Duroudier J.-P., *Crystallization and crystallizers*. (Elsevier, 2016).
- [6] Thomas S., Arif P.M., Gowd E.B., Kalarikkal N., *Crystallization in multiphase polymer systems*. (Elsevier, 2018).
- [7] Paschedag A. R., Computational Fluid Dynamics. in *Ullmann's Encyclopedia of Industrial Chemistry* (Wiley-VCH Verlag GmbH & Co. KGaA, 2005)
- [8] Sawko R., Thompson C., Mathematical and Computational Methods of non-Newtonian, Multiphase Flows. (2011).
- [9] Jones A. G. *Crystallization process systems*. (Butterworth-Heinemann, 2002).
- [10] Rymarczyk T. et al., Practical Implementation of Electrical Tomography in a Distributed System to Examine the Condition of Objects. *IEEE Sens. J.*, 17 (2017), 8166–8186
- [11] Korzeniewska E., Gałazka-Czarnecka I., Czarnecki A., Piekarska A., Krawczyk A., Influence of PEF on antocyanins in wine, *Przegląd Elektrotechniczny*, 94 (2018), No. 1, 57-60.
- [12] Korzeniewska E., Szczesny A., Parasitic parameters of thin film structures created on flexible substrates in PVD process, *Microelectronic Engineering*, 193 (2018), 62-64.
- [13] Rymarczyk T., Kłosowski, G. Application of neural reconstruction of tomographic images in the problem of reliability of flood protection facilities. *Eksploat. i Niezawodn. – Maint. Reliab.* 20 (2018), 425–434
- [14] Rymarczyk T., Kłosowski G., Kozłowski E., A Non-Destructive System Based on Electrical Tomography and Machine Learning to Analyze the Moisture of Buildings. *Sensors*, 18 (2018), 2285
- [15] Kłosowski G. & Rymarczyk T. Using neural networks and deep learning algorithms in electrical impedance tomography. *Inform. Autom. Pomiary w Gospod. i Ochr. Środowiska*, 7 (2017), 99–102
- [16] Borsoi R. A., Aya J. C. C., Costa G. H., Bermudez J. C. M., Super-resolution reconstruction of electrical impedance tomography images. *Comput. Electr. Eng.*, 69 (2018), 1–13